IEEE Access
Multidisciplinary | Rapid Review | Open Access Journal

Received April 12, 2021, accepted April 27, 2021, date of publication May 10, 2021, date of current version May 19, 2021.

Digital Object Identifier 10.1109/ACCESS.2021.3078568

SCMA Codebook Design Based on Divided Extended Mother Codebook

ZHAOYANG HOU, ZHENG XIANG, PENG REN, AND BOHAO CAO
School of Telecommunication Engineering, Xidian University, Xi'an 710071, China
Corresponding author: Zhaoyang Hou (xidian_zhaoyanghou@163.com)

ABSTRACT Sparse code multiple access (SCMA) is one of the competitive non-orthogonal multiple access (NOMA) techniques for the next generation communication systems. In this paper, we put forward a simple and efficient design method named divided extended mother codebook (DEMC) to construct SCMA codebooks based on golden angle modulation (GAM) constellation points. First, we generate a vector defined by the GAM. Second, we design the extended mother codebook (**EMC**) by introducing the power and phase dependent constraints of symbols in multi-dimension codewords. The power constraints can ensure the power of each codeword is the same which leads to the optimal peak to average power ratio (PAPR) especially for the uplink channel. Third, we divide the **EMC** into several mother codebooks (**MC**s) to generate the constant bit rate (CBR) or variable bit rate (VBR) SCMA codebooks. The structure of the VBR SCMA codebooks is compatible with that of CBR. The VBR codebooks and CBR codebooks use the same factor graph, therefore, the users employed the VBR codebooks can also utilize the efficient message passing algorithm (MPA) for multi-user detection. Simulations reveal that the bit error rate (BER) performance of the proposed CBR DEMC-SCMA codebooks is outstanding with low complexity. The VBR DEMC-SCMA codebooks can flexibly satisfy the different service requirements, and the BER performance of the VBR DEMC-SCMA codebooks is close to each other though their modulation orders are various. This feature shows that the users can apply for a high order codebook to get a faster information transfer rate without increasing transmission power and bandwidth.

INDEX TERMS Sparse code multiple access (SCMA), constant bit rate (CBR) codebook, variable bit rate (VBR) codebook, design of dependent multi-dimension codeword.

I. INTRODUCTION

In recent years, the fourth generation (4G) communication using wireless orthogonal access is difficult to effectively meet the rapid development of all multimedia communication services. Therefore, the fifth generation (5g) mobile communication came into being. The spectral efficiency of 5G will be 5∼15 times that of 4G. However, limited by cyclic prefix and orthogonality between sub-carriers, orthogonal frequency division multiplex access (OFDMA) cannot meet the requirements of future 5G system. Driven by this problem, non-orthogonal multiple access, such as sparse code multiple access (SCMA) [1], becomes a hot research topic in recent years.

SCMA is applied to the application scenarios in which multiple users were served on the same time-frequency resource, and it can achieve massive capacity and connectivity [2]. SCMA is a non-orthogonal spread spectrum technology based on multidimensional codebooks, which is similar to the low density signature (LDS) [3]. LDS is a special approach of code division multiple access (CDMA) sequence, and the codewords of LDS are built by the spreading of modulated quadrature amplitude modulation (QAM) symbols using low-density spreading signatures. In SCMA, a dedicated codebook was assigned to each layer/user and incoming bits are mapped into a complex multi-dimension codeword. A plurality of codewords form a codebook [4]. In [5] and [6], several layers/users are multiplexed on the same time-frequency resource to improve the spectral efficiency. The main innovations of SCMA are low-density spreading spectrum and high dimension modulation [7]. Higher dimension modulation can increase the Euclidean distance of the codeword for improving the bit error rate (BER) performance. Similar to LDS system, the main problem of SCMA codebook design is the optimization of complex multi-dimensional constellation. Unfortunately, the

The associate editor coordinating the review of this manuscript and approving it for publication was Zilong Liu.

designing of an optimal SCMA codebook is still an open problem. Hence, a suboptimal method is used for SCMA codebook design [7]–[10].

Combined with constellation rotation in [11], the SCMA codebooks was proposed and designed based on multi-dimensional constellations. In this study, a sub-optimal codebook design was proposed to separate the mother codebook (**MC**) from the operator. The points in the **MC** provided by HUAWEI are distributed on a straight line, and codebooks of users were obtained by executing a simple phase operation on the **MC**. Successive interference cancel (SIC) property was exploited by [4] to separate interfering users by increasing power diversity over interfering codewords which can capture as much as power diversity. Using turbo trellis coded modulation technology, a basic complex multidimensional constellation is designed in [12], which can increase the minimum Euclidean distance. By maximizing the sum-rate, [13] proposed a novel SCMA codebooks design scheme in which a 1-dimensional complex points were used to construct the multi-dimensional constellation sets. Based on star-QAM constellations, [14] proposed a new SCMA codebooks whose BER performance is much better than the codebooks provided in [3]. By executing constellation rotation and interleaving on the quadrature amplitude modulation (QAM) or pulse amplitude modulation (PAM) constellations, [15] proposed a multi-demensional SCMA (MD-SCMA) codebooks design methods for downlink SCMA systems. Similar to the codebook originally proposed by HUAWEI, these symbols are distributed in a line, which provides convenience for optimizing the rotation angle to a certain extent. However, with the increase of the codebook scale, it is bound to lead to a low power efficiency. An optimized 16-point round QAM was divided into several subsets to construct the SCMA codebook in [16]. However, the segmentation procedure is complicated and the rotation angle needs to be optimized, which limits its application in the large-scale codebook. Based on the previous work in [15], [17] constructed SCMA codebooks for uplink and downlink by using the points of golden angle modulation (GAM) constellation. Compared with the proposed codebooks based on constellation rotation and interleaving, the codebooks in [17] exhibits better performance with lower peak to average power ratio (PAPR). [18] proposed a systematic construction method for designing SCMA codebooks in different channel environments. To achieve near-optimal codebooks, several optimal method such as optimized rotation angle, optimized symbols pairing in the codewords, and optimized codeword label had been taken. But, all these optimization measures will increase the computational complexity. [18] also proposed a novel metric of a rotation angle of sub-constellation to find the optimal rotation angle and a cost function of labeling rule to seek the optimal label of codewords. [19] aimed to find an optimized lattice **MC** having large power variation among the constellation points by optimizing the energy and maximum Euclidean distance (MED) alternately. [20] proposed two interference cancellation (IC) related receivers to reduce complexity, including serial interference cancellation (SIC) and jointed serial interference cancellation with message passing algorithm (MPA) algorithm (Jointed SIC-MPA). Both of them have lower complexity compared with the classic MPA receiver. [21] described a sub-optimal modeling of noise using polynomial probability distributions rather than a normal distribution to eliminate the exponential calculations for MPA detectors. The modifying MPA needs much lower computational/hardware complexity reaching the desired BER. The expression of average mutual information (AMI) of SCMA was derived in [22]. [23] studied two types of overloaded code domain NOMA, i.e., dense code multiple access (DCMA) and sparse code multiple access (SCMA). A novel sparse code multiple access (SCMA) scheme named delayed bit-interleaved coded SCMA(DBIC-SCMA) was investigated in [24] and significant improvements in error rate performance was achieved over the classical BIC-SCMA scheme. [25] indicated that the performance of LDS with the aid of Eisenstein number is comparable to that of SCMA in Rayleigh fading channels and better in Gaussian channels than that of SCMA.

Recently, a novel modulation method called GAM was proposed in [26], and the GAM can flexibly adjust the distribution of the constellation points by designing the radius of constellation points. [27] proposed a new geometric shaping design for GAM based on a truncated Gaussian distribution to improve the mutual information (MI). [28] designed geometric- and probabilistic-shaping based GAM scheme to practically overcome the shaping-loss of 1.53 dB compared with QAM. [29] designed a spatial modulation multiple in multiple out (MIMO) communication system based on GAM. To solve the fractional bits problem, a media-based modulation was presented in [30] with golden angle modulation.

In this study, we proposed a divided extended mother codebook (DEMC) to construct SCMA codebooks simply and efficiently based on the GAM. We generate an extended mother codebook (**EMC**) by introduced the power and phase dependence between the symbols in codewords. Then, we divide the **EMC** into several mother codebooks (**MC**s) according to the modulation order M. Last, we label the codeword in **MC**s and assign **MC**s to users. Adaptive rate communication can be more flexible to meet the needs of different channel conditions and services. However, in the traditional codebooks design method, the codebooks employed by all multiplexed users/layers have the same size. We call this kind of codebook as constant bit rate (CBR) codebook, which limits the application of SCMA. In this study, we also use the proposed DEMC method to design variable bit rate (VBR) SCMA codebooks whose scale is various to others. The main contributions of this study are as follows.

- We design an **EMC** which contains all the symbols employed by all resources by introducing the power and phase dependence. Due to the reduction of parameters optimization steps such as rotation, iterativing, maximum Euclidean distance, and maximum produce distance, the DEMC is very simple and efficient. We divide

the **EMC** into several CBR **MC**s and several users use a CBR **MC** to generate the user's codebook.
- We propose four basic principles to design VBR SCMA codebooks.
- Compared with the existing design method which provided CBR SCMA codebooks, we divide the **EMC** into several VBR **MC**s according to the predefined modulation order. The users can apply for codebook with different modulation orders to meet the service requirements. The VBR SCMA codebooks structure can be compatible with the CBR SCMA codebooks structure. They can use the same factor graph, which can utilize the MPA to achieve multi-user detection.

The rest of this paper is arranged as follows. In section II, we briefly review the basic theory of SCMA codebooks design and introduce the GAM. In section III, we propose the DEMC method to design the CBR SCMA codebooks. In section IV, we propose four principles of VBR SCMA codebooks and modify the DEMC to generate the VBR SCMA codebooks. Section V gives the performance simulations of CBR and VBR codebooks proposed in this study. Section VI concludes this paper and prospects the future work.

Notations: Boldface capital and lowercase letters represent the matrices and vectors respectively. The binary, complex and integer field are marked as $\mathbb{B}$, $\mathbb{C}$, and $\mathbb{Z}$ respectively. $CN(0, 1)$ denotes the zero-mean, unit-variance, circularly symmetric, and complex Gaussian distribution. Superscript *, ^{T}, and ^{H} denote the conjugate, transpose, and conjugate transpose respectively. $|\cdot|$ denotes the norm of a complex vector or scalar. $\mathbf{I}_n$ denotes $n \times n$ unit matrix. $\mathbf{A}^{(k)}$ denotes the k-th $\mathbf{A}$. $\mathbf{A}_{k,:}$ and $\mathbf{A}_{:,k}$ respectively denote the k-th row and k-th column of $\mathbf{A}$. diag($\mathbf{A}$) denotes the vector of diagonal elements of $\mathbf{A}$. diag($\mathbf{x}$) denotes the squire matrix whose diagonal elements is $\mathbf{x}$. $\angle\mathbf{x}$ returns the phase of $\mathbf{x}$. * represents the dot product operator. fliplr($\mathbf{x}$) means flip $\mathbf{x}$ left to right. Hamm(a, b) denotes the Hamming distance between label a and b.

In order to make it clear for readers to understand this paper, we stipulate the following habits in advance. A codebook is a complex matrix and is formed by several codewords. A codeword is a complex column vector and is formed by several symbols or constellation points. Unless otherwise specified, user is equivalent to user node (UN) and resource is equivalent to resource node (RN).

II. PRELIMINARY BACKGROUNDS REVIEW AND SYSTEM MODEL

A. SPARSE CODE MULTIPLE ACCESS ENCODING AND MULTIPLEXING

Considering an uplink SCMA system as shown in Fig.1 which consists J UNs and K RNs ($K < J$), e.g., K OFDMA tones, K time slots, …. Each UN is able to access N RNs ($N < K$), while each RN is shared by df UNs ($df < J$). Each UN employed a K-dimensional SCMA codebook which is unique and allocated before communication.

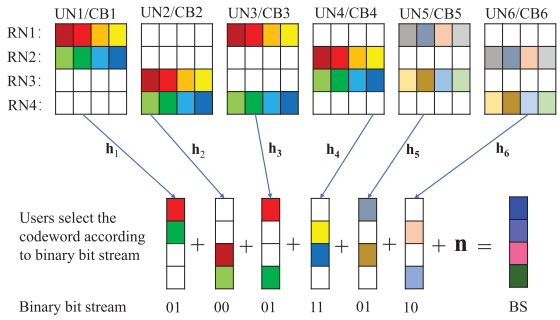

FIGURE 1. SCMA system model for uplink channel.

Each codebook has M codewords and each codeword occupies K RNs. An SCMA encoder is the combination of QAM mapper and spreading signature [1] and is defined as a mapping

$$f_j : \mathbb{B}^{(\log_2 M)\times 1} \rightarrow \mathcal{X}_j, \tag{1}$$

where $\mathcal{X}_j \subset \mathbb{C}^{K\times M}$ is the codebook of j-UN. The incoming vector $\mathbf{b}$ with $\log_2 M$ bits is mapped into a K-dimensional codeword $\mathbf{x} = f_j(\mathbf{b})$ which is selected from the column vector of $\mathcal{X}_j$. Each codeword $\mathbf{x}$ has N non-zero symbols which indicated the codeword is sparse. Due to the sparsity of the codeword, the number of conflicting UNs on the same RN is limited. This feature not only reduces the interference of non-orthogonal users, but also reduces the complexity of multi-user detection.

Define $\mathbf{c}$ as a column vector which contains the non-zeros element in codeword $\mathbf{x}$. The vector $\mathbf{c}$ belongs to a N-dimensional constellation $\mathcal{C}_j \subset \mathbb{C}^{N\times M}$ and the symbols on each dimension can be selected form QAM, PSK, and GAM as shown in Fig.3, …. The mapping from $\mathbb{B}^{\log_2 M}$ to $\mathcal{C}_j$ is written as follows [17],

$$g_j : \mathbb{B}^{(\log_2 M)\times 1} \rightarrow \mathcal{C}_j, \tag{2}$$

such that $\mathbf{c}_j = g_j(\mathbf{b}_j)$. Then the SCMA encoder in (1) can be redefined as $f_j = \mathbf{V}_j \cdot g_j$ where $\mathbf{V}_j \in \mathbb{B}^{K\times N}$ is the binary spreading matrix.

Similar to LDS, SCMA also uses the factor graph to indicate the relationship between the UNs and RNs. The factor graph used in this paper is shown in Fig.2. The factor graph can also be represented by the following matrix,

$$\mathbf{F} = (\mathbf{f}_1, \ldots, \mathbf{f}_J) \subset \mathbb{B}^{K\times J}. \tag{3}$$

where $\mathbf{f}_j = \text{diag}(\mathbf{V}_j\mathbf{V}_j^H)$. The k-RN is used by j-UN if and only if $\mathbf{F}_{k,j} = 1$. So, the factor graph is equivalent to the factor graph matrix. An SCMA system also supports overloading, so that the number of UN can be larger than that of RN, that is, J is larger than K. $\lambda = \frac{J}{K}$ is defined as the overloading factor. For the case of $K = 4$, $J = 6$, and $N = 2$, a possible

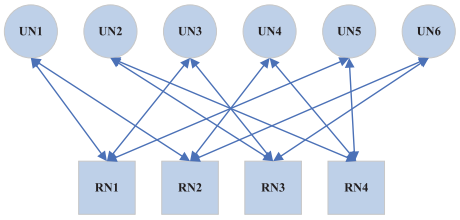

FIGURE 2. Factor graph. UN will occupy RN if UN and RN are connected.

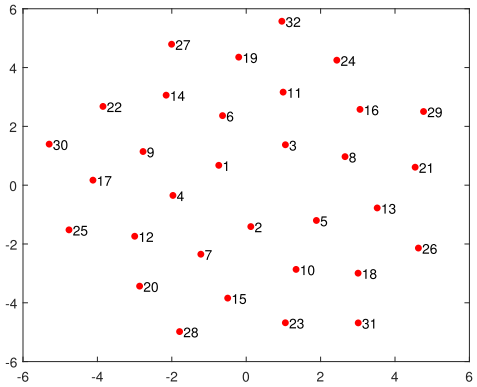

FIGURE 3. GAM constellation with 32 points.

factor graph matrix can be defined as [31],

$$\mathbf{F} = \begin{bmatrix} 1 & 0 & 1 & 0 & 1 & 0 \\ 1 & 0 & 0 & 1 & 0 & 1 \\ 0 & 1 & 1 & 0 & 0 & 1 \\ 0 & 1 & 0 & 1 & 1 & 0 \end{bmatrix}. \tag{4}$$

The corresponding spread spectrum matrix for 1-UN and 2-UN are defined as follows,

$$\mathbf{V}_1 = \begin{bmatrix} 1 & 0 \\ 0 & 1 \\ 0 & 0 \\ 0 & 0 \end{bmatrix}, \mathbf{V}_2 = \begin{bmatrix} 0 & 0 \\ 0 & 0 \\ 1 & 0 \\ 0 & 1 \end{bmatrix}, \mathbf{V}_3 = \begin{bmatrix} 1 & 0 \\ 0 & 0 \\ 0 & 1 \\ 0 & 0 \end{bmatrix},$$
$$\mathbf{V}_4 = \begin{bmatrix} 0 & 0 \\ 1 & 0 \\ 0 & 0 \\ 0 & 1 \end{bmatrix}, \mathbf{V}_5 = \begin{bmatrix} 1 & 0 \\ 0 & 0 \\ 0 & 0 \\ 0 & 1 \end{bmatrix}, \mathbf{V}_6 = \begin{bmatrix} 0 & 0 \\ 0 & 1 \\ 1 & 0 \\ 0 & 0 \end{bmatrix}. \tag{5}$$

The constellation operators g_j generally include phase rotation, coordinate interleaving, complex conjugate, and dimensional permutation.

In the uplink, the received signal at the base station (BS) can be defined as

$$\mathbf{r} = \sqrt{\frac{E_s}{df}} \sum_{j=1}^{J} \text{diag}(\mathbf{h}_j)\mathbf{x}_j + \mathbf{n}, \tag{6}$$

where E_s represents the average power of the transmitted symbols. $\mathbf{h}_j = (h_{1,j}, \ldots, h_{K,j})^T \in \mathbb{C}^{K\times 1}$ denotes the channel vector from the j-th UN to the BS and $h_{k,j} \sim CN(0,1)$. $\mathbf{n} = (n_1, \ldots, n_K)$ denotes the noise vector at the BS and $n_k \sim CN(0, N_0)$ is the complex AWGN. The block diagrams for the uplink system is shown in Fig.1. The PAPR of a codebook $\mathcal{X}_j$ is defined as

$$PAPR[dB] = 10\log_{10}\left(\frac{\max\limits_{1\le m\le M}\left(\sum_{k=1}^{K}|\mathcal{X}_{k,m}|^2\right)}{E}\right),$$
$$E = \frac{1}{M}\sum_{m=1}^{M}\sum_{k=1}^{K}|\mathcal{X}_{k,m}|^2. \tag{7}$$

B. GOLDEN ANGLE MODULATION

The golden angle modulation (GAM) is defined as follows in [26],

$$y_n = r_n e^{j2\pi\varphi n}, \quad n \in \{1, 2, \ldots, N\}, \tag{8}$$

where y_n and r_n denote the complex amplitude and the radius of the n-th constellation point. $2\pi\varphi n$ is the phase angle of n-th constellation point. $\varphi = \frac{3-\sqrt{5}}{2}$ is the golden angle in rads. Fig.3 shows a disc-GAM constellation with $r_n = \sqrt{n}, n = \{1, 2, \ldots, 32\}$. GAM features the following advantages. 1) Natural constellation point index: Compared with other modulation such as QAM, APSK without any natural index order, GAM enables a unique index $n \in 1, 2, \ldots N$. 2) Almost near-ideal circular design: Circular design can provide advanced MI-, distance-, symbol error rate- and PAPR- performance over other constellations. 3) Any number of constellation points, while keeping the overall circular shape: This gives more flexibility, for example, controllable number of constellation. More details about GAM is illustrated in [26]–[28]. In this paper, we design SCMA codebooks based on disc-GAM which is defined as follows,

$$r_n = c_{disc}\sqrt{n}, \quad n \in \{1, 2, \ldots, N\},$$
$$c_{disc} = \sqrt{\frac{2\bar{P}}{N+1}}. \tag{9}$$

where $\bar{P}$ denotes the average power of the constellation. Here, $\bar{P}$ can be any positive number, because the codebook will be normalized in next step.

III. CONSTANT BIT RATE SCMA CODEBOOKS DESIGN BASED ON GAM

In this section, we will design a CBR SCMA codebook for the AWGN channel and Rayleigh fading channel. Considering the system parameters $K = 4, J = 6, N = 2$, and $M = 4$, the codeword matrix (**CM**) can be used to describe the following design idea.

$$\mathbf{CM} = \begin{bmatrix} \mathbf{y}_1 & 0 & \mathbf{y}_2 & 0 & \mathbf{y}_3 & 0 \\ \mathbf{y}_4 & 0 & 0 & \mathbf{y}_2 & 0 & \mathbf{y}_3 \\ 0 & \mathbf{y}_1 & \mathbf{y}_5 & 0 & 0 & \mathbf{y}_6 \\ 0 & \mathbf{y}_4 & 0 & \mathbf{y}_5 & \mathbf{y}_6 & 0 \end{bmatrix}, \tag{10}$$

where $\mathbf{y}_1, \mathbf{y}_2, \ldots, \mathbf{y}_6$ represent sub-vectors which are derived from $\mathbf{y}$ by splitting and rotating. Each row/RN of **CM** employees $df = \frac{JN}{K} = 3$ sub-vectors and each column/UN contains $N = 2$ sub-vectors. It is noticed that every two UNs

employ the same sub-vectors and this feature will contribute to design variable bit rate (VBR) codebooks which will be introduced in next section. The detailed design procedure of CBR SCMA codebooks is given as follows.

A. GENERATION OF MOTHER BOOK (MC)

1) Generate a vector $\mathbf{y} = \{y_{np} | np = 1, 2, \ldots, NP\}$ where $NP = (M_1 + M_2 + M_{df})/2$ based on GAM according to (8) and (9).
2) The symbols employed by the resources/dimensions is generated by rotating the vector $\mathbf{y}$ according to (11).

$$\mathbf{Y}_{n,:} = \mathbf{y} * e^{j\frac{n-1}{N}}, n \in \{1, 2, \ldots, N\}. \tag{11}$$

3) Introduce dependence of power and phase between the dimensions according to (12).

$$\mathbf{Y}_{n+\frac{N}{2},:} = \angle \mathbf{Y}_{n,:} * \text{fliplr}\left(\left|\mathbf{Y}_{n+\frac{N}{2},:}\right|\right), \quad n \in \{1, 2, \ldots, \frac{N}{2}\}. \tag{12}$$

4) Generate the other half symbols marked as $\mathbf{Y}' = -\mathbf{Y}$.
5) Generate the **EMC** by rearranging the symbols in $\mathbf{Y}'$ and $\mathbf{Y}$ according to (13).

$$\begin{aligned} \mathbf{EMC}_{:,1:2:NP*2} &= \mathbf{Y} \\ \mathbf{EMC}_{:,2:2:NP*2} &= \mathbf{Y}'. \end{aligned} \tag{13}$$

6) Divide the **EMC** to a few of **MC**s according to (14) ensuring the size of each **MC** is the same, which leads that the transmission rate of all users are the same. This is why this kind of codebook is called CBR codebook. In this step, those opposite numbers are arranged in a codebook to increase the Euclidean distance between codewords. On the contrary, if those opposite numbers are assigned in different codebooks, a few superimposed symbols at the receiver may be the same, which will be confusing for demodulating.

$$\mathbf{MC}^{(k)} = \mathbf{EMC}_{:,(k-1)*M+1:k*M}. \tag{14}$$

where $k = \{1, 2, \ldots, df\}$ denotes k-th **MC**.
7) Codebook energy normalization.

$$\begin{aligned} \mathbf{MC}^{(k)} &= \frac{\mathbf{MC}^{(k)}}{\sqrt{P^{(k)}}}, \\ P^{(k)} &= \sum_{n=1}^{N}\sum_{m=1}^{M}\left|\mathbf{MC}^{(k)}_{n,m}\right|^2. \end{aligned} \tag{15}$$

B. GENERATION OF USER CODEBOOK

In order to improve the BER performance, [18] further pairs the symbols between different resources/dimensions in a codeword of an **MC** based on maximum Euclidean distance (MED) metric or maximum product distance (MPD) metric and finds the optimal solution by trying all the possible combinations. The brute force (BF) strategy will consume a huge amount of computation $df * (M!)^{N-1}$, which is unreachable with the increase of the codebooks scale. However, we pair the symbols to introduce the power and phase dependence which greatly reduces the complexity. This is similar to the spread spectrum technology introduced in CDMA which can further improve the BER performance. Combined with those spread spectrum matrix provided in (5), we can get the user codebook (**UCB**).

$$\mathbf{UCB}^{(j)} = \mathbf{V}^{(j)} * \mathbf{MC}^{\left(\left\lfloor \frac{(j-1)*df}{J} + 1 \right\rfloor\right)}. \tag{16}$$

where $\lfloor x \rfloor$ denotes the floor function of x and $j \in \{1, 2, \ldots, J\}$.

So far, we get all **UCB**s. Moreover, for each **UCB**, we construct its M codewords. Next, we will define the label for each codeword. In general, Gray mapping is considered to be the best labeling rule [32], because the Hamming distance between the nearest constellation points is 1. But the Gray mapping is not suitable for the SCMA codebooks. Based on the binary switch algorithm (BSA) proposed in [18], [33] probosed a BSA-based labeling rule. The BSA-based labeling rule tries to find the codeword label that minimizes the objective cost function by switching the label of codewords. The complexity is $\mathcal{O}(\frac{dfM^4}{2})$. Compared with the BF method whose complexity is $\mathcal{O}(df * M!)$, BSA makes a trade-off between performance and complexity. So, in this paper, we use BSA to get the label of codewords. Algorithm 1 shows the labeling rule for the AWGN channel. For the Rayleigh fading channel, we just need to change the Euclidean distance (ED) to product distance (PD). In practical application, we run BSA several times to get feasible labels of the codewords.

Algorithm 1 Labeling Rule of SCMA Codebooks Based on BSA for AWGN Channel

Input: **MC** and M.
Initialize $L = \{0, 1, \ldots, M-1\}$
for $m = 1 : M-1$ **do**
  for $n = m+1 : M$ **do**
    Calculate the $ED_{m,n}$ between $\mathbf{MC}_{:,m}$ and $\mathbf{MC}_{:,n}$.
  end for
end for
for $m = 1 : M-1$ **do**
  for $n = m+1 : M$ **do**
    Calculate $C_L = \sum_{i=1}^{M-1}\sum_{j=i+1}^{M} \text{Hamm}(L_i, L_j)e^{-ED_{i,j}}$.
    Switch the L_m and L_n in L.
    Calculate $C_{sL} = \sum_{i=1}^{M-1}\sum_{j=i+1}^{M} \text{Hamm}(L_i, L_j)e^{-ED_{i,j}}$.
    if $C_{sL} > C_L$ **then**
      Switch the L_m and L_n in L.
    end if
  end for
end for
Output: L

Assuming the system parameters are $K = 4$, $J = 6$, $N = 2$, $M_1 = M_2 = M_3 = M_4 = M_5 = M_6 = 8$. Table 1 shows the emample of **EMC** for CBR SCMA codebooks and table 2 shows the example of **MC**s for CBR SCMA codebooks. The detailed CBR SCMA codebooks is provided in appendix-A and the performance is estimated in section V.

TABLE 1. Example of EMC for CBR SCMA codebooks.

index		$\mathbf{EMC}_1$	$\mathbf{EMC}_2$	$\mathbf{EMC}_3$	$\cdots$	$\mathbf{EMC}_{23}$	$\mathbf{EMC}_{24}$
dim-1	norm	$\lvert y_1\rvert$[a]	$\lvert y_1\rvert$	$\lvert y_2\rvert$	$\cdots$	$\lvert y_{12}\rvert$[c]	$\lvert y_{12}\rvert$[d]
	phase	$2\pi\varphi$	-$2\pi\varphi$[b]	$4\pi\varphi$	$\cdots$	$24\pi\varphi$[c]	-$24\pi\varphi$[d]
dim-2	norm	$\lvert y_{12}\rvert$[a]	$\lvert y_{12}\rvert$	$\lvert y_{11}\rvert$	$\cdots$	$\lvert y_1\rvert$	$\lvert y_1\rvert$
	phase	$2\pi\varphi$	-$2\pi\varphi$[b]	$4\pi\varphi$	$\cdots$	$24\pi\varphi$	-$24\pi\varphi$

[a] : Each column of **EMC** contains the non-zero symbols in a codeword. The power of each column of **EMC** is equal to $NP + 1$ which leads to the optimal PAPR, that is, the PAPR of each codeword is 1. Furthermore, this is an important feature that indicates the dependence of different symbols in a codeword. This feature can further improve the performance against noise and channel fading.
[b] : The symbols in each column of **EMC** have the same phase. This feature can equalize the phase noise and help the receiver to detect and correct the noise and channel fading.
[c,d] : The opposite numbers are arranged in every codebook to increase the Euclidean distance or product distance of codewords.

TABLE 2. Example of MC of CBR SCMA codebooks.

$\mathbf{MC}^{(1)}$	$\mathbf{MC}^{(2)}$	$\mathbf{MC}^{(3)}$
$\mathbf{EMC}_1,\cdots,\mathbf{EMC}_8$	$\mathbf{EMC}_9,\cdots,\mathbf{EMC}_{16}$	$\mathbf{EMC}_{17},\cdots,\mathbf{EMC}_{24}$

Every M columns of **EMC** form an **MC**. All **MC** have the same scale which results in the same information transmission rate.

IV. VARIABLE BIT RATE SCMA CODEBOOK DESIGN BASED ON GAM

In an adaptive information transmission rate communication system, variable bit rate (VBR) codebooks can satisfy the service requirement flexibly. However, the traditional SCMA codebooks only provide CBR codebooks which are deduced from the single **MC**. In order to design the VBR codebooks, we abandon the existing SCMA codebook design procedure and utilize the DEMC to construct a novel codebooks with different modulation order which can provide various transmission rates. In order to be compatible with the traditional SCMA codebooks, the new codebook design method follows the four principles below.

1) Principle-1: The number of symbols employed by each resource is the same.
2) Principle-2: Introduce a parameter $\gamma = \frac{K}{N}$. The value of K and N should satisfy that γ is an integer. γ denotes the group size and will be helpful to divide the **EMC** for the design of VBR SCMA codebooks.
3) Principle-3: All users are divided into several groups. Users divided into a group should have the same modulation order.
4) Principle-4: The VBR SCMA uses the same factor graph as CBR SCMA.

Algorithm 2 : Design Procedure of VBR SCMA Codebooks

Input: N, K, J and $M_j, j \in \{1, 2, \ldots, J\}$
1: Calculate $\gamma = \frac{K}{N}$ and $df = \frac{J}{\gamma}$.
2: Divide the users into df groups according the modulation order.
3: Calculate number of constellation points $NP = (\sum_{k=1}^{J} M_k) * N/K/2$.
4: Generate a vector $\mathbf{y}$ with NP elements according (8).
5: Generate **EMC** according to (12) and (13)'
6: **for** $k = 1$ to df **do**
7: Generate $\mathbf{MC}^{(k)}$ according to (17).
8: **end for**
9: **for** $j = 1$ to J **do**
10: Generate $\mathbf{UCB}^{(j)}$ according to (16).
11: **end for**
12: Label the codewords in the **MC**s according Algorithm 1.
Output: $\mathbf{UCB}^{(j)}, j = \{1, 2, \ldots, J\}$

Compared with the design of CBR SCMA codebooks, we can design the VBR SCMA codebooks with a few modifications. Algorithm 2 shows the design procedure of VBR SCMA codebooks. Since one user does not occupy all the resources which are determined by the factor graph. If we set the modulation order of user arbitrarily, the number of constellation points employed by each RN will not be equal which increases the design complexity of codebooks. So, we propose the principles above to limit the number of users and modulation order. As a result, the total number of symbols employed by each resource is the same. The variable $\gamma = \frac{K}{N}$ represents the minimum group size. The number of groups is $\frac{JN}{K}$ which is equal to df. The codewords matrix shown in (10) shows the feasibility of this idea if every two users form a group. Table 3 shows the difference of symbol assignment between CBR and VBR.

The design procedure of VBR SCMA codebooks is similar to the design procedure of CBR except the (14). Here, we redefine the segmentation procedure in (17).

$$\mathbf{MC}^{(k)} = \mathbf{EMC}_{:,1+\sum_{a=1}^{k-1} M_{a*K/N}:\sum_{a=1}^{k} M_{a*K/N}}, \tag{17}$$

where $k = \{1, 2, \ldots, df\}$ and $\sum_{a=1}^{0} M_{a*K/N} = 0$.

It is noticed that NP is some discrete integers, but it is usually not an integer power of 2. So, most of the constellations could not provide suitable symbols. However, the feature-3 of GAM indicates that the number of the GAM constellation can be any integer, which perfectly meets the number requirement of VBR SCMA codebooks. This is why the GAM is selected to construct the VBR SCMA codebooks.

Since the VBR codebooks use the same factor graph as CBR, we can use the pure MPA to demodulate the multi-user data with a little modification, which is not described here. Once the VBR codebooks are generated, in practical application, users can apply for different codebooks according to their service requirements. In special cases, users can

TABLE 3. Comparison of symbol assignment of CBR and VBR codebooks.

Codebook	Resource	Group-1		Group-2		Group-3		Total
		U1	U2	U3	U4	U5	U6	
CBR	RN1	8[a]	0	8[a]	0	8[a]	0	24[e]
	RN2	8	0	0	8[d]	0	8	24[e]
	RN3	0	8	8	0	0	8	24[e]
	RN8	0	8	0	8[d]	8	0	24[e]
VBR	RN1	4[b,c]	0	8[b]	0	16[b]	0	28[f]
	RN2	4[c]	0	0	8[d]	0	16	28[f]
	RN3	0	4[c]	8	0	0	16	28[f]
	RN4	0	4[c]	0	8[d]	16	0	28[f]

[a] : The number of symbols employed by users on each resource is the same for CBR codebooks.
[b] : The number of symbols employed by users in different groups on each resource is various for VBR codebooks.
[c] : The number of symbols employed by users in the same group is the same for VBR codebooks.
[d] : The resources occupied by CBR and VBR codebooks are the same, which indicates the factor graph used by CBR and VBR codebooks are the same. This will help VBR codebooks to introduce efficient multi-user detection approach such as MPA.
[f] : The total number of symbols employed by each resource is the same for VBR codebooks.
[e,f] : Usually, the total number of VBR and CBR SCMA codebooks is different. The performance comparison of the two codebooks will be given in the next section.

even allocate multiple codebooks to meet the requirements of higher rate communication.

Assuming the system parameters are $K = 4$, $J = 6$, $N = 2$, $M_1 = M_2 = 4$, $M_3 = M_4 = 8$, and $M_5 = M_6 = 16$. Table 4 shows the emample of **EMC** for VBR SCMA codebooks and table 5 shows the example of **MC**s for VBR SCMA codebooks. The detailed VBR SCMA codebooks is provided in appendix-A and the performance is estimated in section V.

TABLE 4. Example of EMC for VBR SCMA codebooks.

index		$\mathbf{EMC}_1$	$\mathbf{EMC}_2$	$\mathbf{EMC}_3$	$\cdots$	$\mathbf{EMC}_{27}$	$\mathbf{EMC}_{28}$
dim-1	norm	$\lvert y_1\rvert$[a]	$\lvert y_1\rvert$	$\lvert y_2\rvert$	$\cdots$	$\lvert y_{14}\rvert$	$\lvert y_{14}\rvert$
	phase	$2\pi\varphi$	$-2\pi\varphi$[b]	$4\pi\varphi$	$\cdots$	$28\pi\varphi$	$-28\pi\varphi$
dim-2	norm	$\lvert y_{14}\rvert$[a]	$\lvert y_{14}\rvert$	$\lvert y_{13}\rvert$	$\cdots$	$\lvert y_1\rvert$	$\lvert y_1\rvert$
	phase	$2\pi\varphi$	$-2\pi\varphi$[b]	$4\pi\varphi$	$\cdots$	$28\pi\varphi$	$-28\pi\varphi$

TABLE 5. Example of MCs for VBR SCMA codebooks.

$\mathbf{MC}^{(1)}$	$\mathbf{MC}^{(2)}$	$\mathbf{MC}^{(3)}$
$\mathbf{EMC}_1,\cdots,\mathbf{EMC}_4$	$\mathbf{EMC}_5,\cdots,\mathbf{EMC}_{12}$	$\mathbf{EMC}_{13},\cdots,\mathbf{EMC}_{28}$

Every 4, 8, and 16 columns of **EMC** form an **MC**. The size of the **MC**s may be different which can carry different amounts of information.

V. SIMULATION RESULTS AND ANALYSIS

In this section, we give the simulations considering the cases where $J = 6$, $K = 4$, and $N = 2$. The factor graph in Fig.2 and the corresponding factor graph matrix given in (4) are adopted to generate the codebooks. The number of iterations of MPA is set to 6. The BSA is run 20 times to optimize the codeword label. The BER performance of CBR and VBR SCMA codebooks is estimated based on the example above for AWGN channel and Rayleigh fading channel. We also compare the computational complexity and BER performance of previous designs such as MD-SCMA proposed in [15], GAM-SCMA proposed in [17], and MUO-SCMA proposed in [18].

Generally, the complexity of demodulation algorithm of SCMA codebook have attracted more attention. However, we also should pay attention to the design complexity of SCMA codebooks. Table 6 gives the comparison of design complexity about rotation, interleaving, MED/MPD, dependence, and label. Obviously, the design complexity of MUO-SCMA is the highest, because its each step uses brute force (BF) to optimize the parameters. The factorial operation is not unreachable with the increase of codebooks scale. That is to say, higher order codebooks cannot be designed, such as $M = 16$. Similar to MUO-SCMA, the GAM-SCMA also uses the BF to optimize the rotation angle, but the design complexity is lower than it. The MD-SCMA and the DEMC-SCMA have the lowest design complexity.

TABLE 6. Comparison of design complexity of different designs.

Codebook	MD	GAM	MUO	DEMC
Rotation	little[a]	180^{df-1}	180^{df-1}	little
Interleaving	little	little	none	none
Dependence	none[b]	none	none	little
MED/MPD	none	none	$df(M!)^{N-1}$,[c]	none
Label	little	little	$\frac{df}{2}M^4$	$\frac{df}{2}M^4$

[a] : "little" means the operation requires a little computation.
[b] : "none" means no such operation is adopted.
[c] : The complexity of factorial operation will increase explosively with the increase of codebooks scale, which can not be realized.

Fig.4 shows the BER performance for the uplink AWGN channel. The MD-SCMA performs the worst because the symbols employed by MD-SCMA are distributed on a line. Compared with other design schemes, the symbols of linear distribution waste more energy. The GAM with

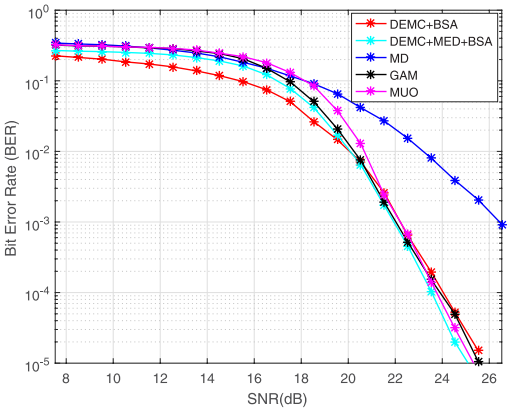

FIGURE 4. Comparison of BER performance versus the SNR for the uplink AWGN channel where M = 8.

near-idea circular constellation points has the nature advantage over symbol energy. The performance of GAM-SCMA, MUO-SCMA, and DEMC-SCMA codebooks is similar in the high SNR region, but in the low SNR region, the DEMC-SCMA codebooks perform the best. Compared the red curve with the cyan curve, we also find that though the Euclidean distance of the codewords can be maximized by exchanging symbols with other codewords, the improvement of BER performance is limited.

Though multidimensional codewords can achieve diversity gain, no efficient measures have been taken to achieve the diversity gain in practice. These papers only increase the product distance or Euclidean distance between codewords by switch the symbols employed by each resource which brings enormous complexity. By introducing dependence between symbols on different dimensions in the codeword, the above optimization operation can be avoided. Concurrently, the correlation of symbols in different dimensions of codeword can effectively against channel fading and AWGN.

Fig.5 shows the BER performance for the Rayleigh fading channel. Similar to the BER performance for AWGN channel, the MD-SCMA performs the worst. In the low SNR region, the performance of the five codebooks is close to each other, and the DEMC-SCMA performs best. In the high SNR region, the MUO-SCMA performs the best. Though the cyan curve has an outstanding performance, but the complexity of the MPD limits its application for large scale codebooks like the MUO-SCMA codebooks. As analyzed above, the BER performance can also be improved by taking advantage of the dependence between the symbols in codewords.

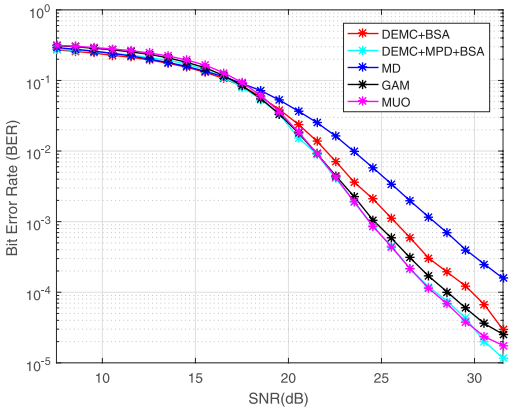

FIGURE 5. Comparison of BER performance versus the SNR for the uplink Rayleigh fading channel where M = 8.

Fig.6 show the SER performance of the VBR SCMA codebooks. In the low SNR region, the SER performance of the codebook of $M = 4$ is the best, because the codebook has fewer codewords and the probability of misjudgment is lower. In the high SNR region, the SER performance of the codebook of $M = 4$ and $M = 8$ is the same and is close to that of $M = 16$ due to the power of each codeword is the same.

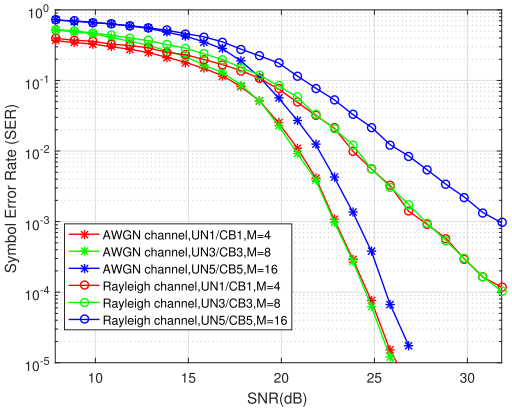

FIGURE 6. SER performance of VBR SCMA codebooks versus the SNR for the uplink AWGN channel and Rayleigh fading channel. The modulation orders of UN1, UN3, and UN5 are 4, 8, and 16.

Fig.7 and Fig.8 shows BER performance of VBR and CBR codebooks. Compared with the BER performance of CBR SCMA codebooks with different modulation, no matter for the AWGN channel or the Rayleigh fading channel, the BER performance of the codebooks with different

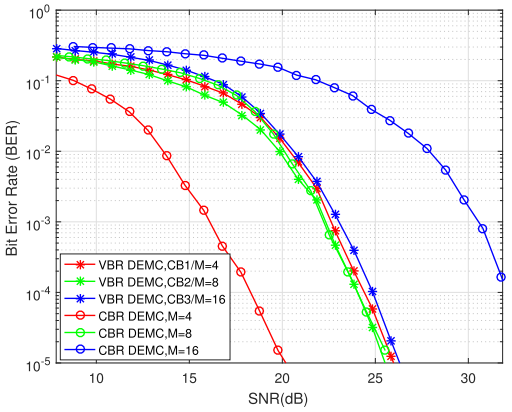

FIGURE 7. Comparison of BER performance of VBR and CBR SCMA codebooks versus the SNR for the uplink AWGN channel.

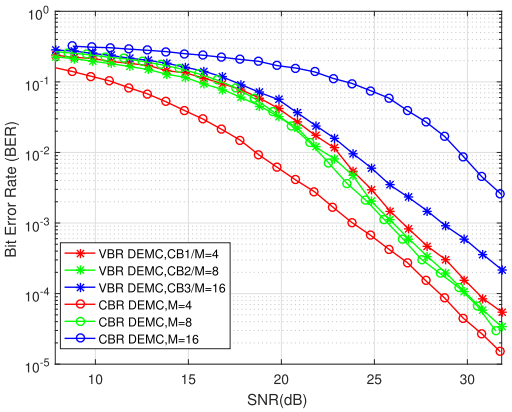

FIGURE 8. Comparison of BER performance of VBR and CBR SCMA codebooks versus the SNR for the uplink Rayleigh fading channel.

modulation orders is close to each other, which is similar to the SER performance. This phenomenon proves that users can apply for codebook with high modulation order to achieve faster information transmission rate keeping the constant

$$\mathcal{X}_1: \begin{bmatrix} 0.1033-0.1348i & 0.1887-0.2461i & 0.0000+0.0000i & 0.0000+0.0000i \\ -0.0121-0.1381i & -0.2897+0.0512i & 0.0000+0.0000i & 0.0000+0.0000i \\ 0.0121+0.1381i & 0.2897-0.0512i & 0.0000+0.0000i & 0.0000+0.0000i \\ -0.1033+0.1348i & -0.1887+0.2461i & 0.0000+0.0000i & 0.0000+0.0000i \\ -0.1931+0.0342i & -0.0284-0.3240i & 0.0000+0.0000i & 0.0000+0.0000i \\ 0.0723+0.0662i & -0.2505-0.2295i & 0.0000+0.0000i & 0.0000+0.0000i \\ -0.0723-0.0662i & 0.2505+0.2295i & 0.0000+0.0000i & 0.0000+0.0000i \\ 0.1931-0.0342i & 0.0284+0.3240i & 0.0000+0.0000i & 0.0000+0.0000i \end{bmatrix}^H$$

$$\mathcal{X}_2: \begin{bmatrix} 0.0000+0.0000i & 0.0000+0.0000i & 0.1033-0.1348i & 0.1887-0.2461i \\ 0.0000+0.0000i & 0.0000+0.0000i & -0.0121-0.1381i & -0.2897+0.0512i \\ 0.0000+0.0000i & 0.0000+0.0000i & 0.0121+0.1381i & 0.2897-0.0512i \\ 0.0000+0.0000i & 0.0000+0.0000i & -0.1033+0.1348i & -0.1887+0.2461i \\ 0.0000+0.0000i & 0.0000+0.0000i & -0.1931+0.0342i & -0.0284-0.3240i \\ 0.0000+0.0000i & 0.0000+0.0000i & 0.0723+0.0662i & -0.2505-0.2295i \\ 0.0000+0.0000i & 0.0000+0.0000i & -0.0723-0.0662i & 0.2505+0.2295i \\ 0.0000+0.0000i & 0.0000+0.0000i & 0.1931-0.0342i & 0.0284+0.3240i \end{bmatrix}^H$$

$$\mathcal{X}_3: \begin{bmatrix} -0.1850-0.1177i & 0.0000+0.0000i & 0.2060-0.0752i & 0.0000+0.0000i \\ 0.1196-0.2302i & 0.0000+0.0000i & 0.0674+0.2505i & 0.0000+0.0000i \\ 0.2605-0.0951i & 0.0000+0.0000i & 0.1107-0.2132i & 0.0000+0.0000i \\ 0.0624+0.2320i & 0.0000+0.0000i & 0.2340+0.1489i & 0.0000+0.0000i \\ -0.0624-0.2320i & 0.0000+0.0000i & -0.2340-0.1489i & 0.0000+0.0000i \\ -0.2605+0.0951i & 0.0000+0.0000i & -0.1107+0.2132i & 0.0000+0.0000i \\ -0.1196+0.2302i & 0.0000+0.0000i & -0.0674-0.2505i & 0.0000+0.0000i \\ 0.1850+0.1177i & 0.0000+0.0000i & -0.2060+0.0752i & 0.0000+0.0000i \end{bmatrix}^H$$

$$\mathcal{X}_4: \begin{bmatrix} 0.0000+0.0000i & -0.1850-0.1177i & 0.0000+0.0000i & 0.2060-0.0752i \\ 0.0000+0.0000i & 0.1196-0.2302i & 0.0000+0.0000i & 0.0674+0.2505i \\ 0.0000+0.0000i & 0.2605-0.0951i & 0.0000+0.0000i & 0.1107-0.2132i \\ 0.0000+0.0000i & 0.0624+0.2320i & 0.0000+0.0000i & 0.2340+0.1489i \\ 0.0000+0.0000i & -0.0624-0.2320i & 0.0000+0.0000i & -0.2340-0.1489i \\ 0.0000+0.0000i & -0.2605+0.0951i & 0.0000+0.0000i & -0.1107+0.2132i \\ 0.0000+0.0000i & -0.1196+0.2302i & 0.0000+0.0000i & -0.0674-0.2505i \\ 0.0000+0.0000i & 0.1850+0.1177i & 0.0000+0.0000i & -0.2060+0.0752i \end{bmatrix}^H$$

$$\mathcal{X}_5: \begin{bmatrix} 0.1314+0.2809i & 0.0000+0.0000i & 0.0000+0.0000i & 0.0720+0.1538i \\ -0.0973+0.3103i & 0.0000+0.0000i & 0.0000+0.0000i & -0.1813-0.0748i \\ 0.2719+0.1122i & 0.0000+0.0000i & 0.0000+0.0000i & 0.0415-0.1323i \\ -0.2939+0.1703i & 0.0000+0.0000i & 0.0000+0.0000i & 0.0848-0.0492i \\ 0.0973-0.3103i & 0.0000+0.0000i & 0.0000+0.0000i & 0.1813+0.0748i \\ -0.1314-0.2809i & 0.0000+0.0000i & 0.0000+0.0000i & -0.0720-0.1538i \\ 0.2939-0.1703i & 0.0000+0.0000i & 0.0000+0.0000i & -0.0848+0.0492i \\ -0.2719-0.1122i & 0.0000+0.0000i & 0.0000+0.0000i & -0.0415+0.1323i \end{bmatrix}^H$$

$$\mathcal{X}_6: \begin{bmatrix} 0.0000+0.0000i & 0.0720+0.1538i & 0.1314+0.2809i & 0.0000+0.0000i \\ 0.0000+0.0000i & -0.1813-0.0748i & -0.0973+0.3103i & 0.0000+0.0000i \\ 0.0000+0.0000i & 0.0415-0.1323i & 0.2719+0.1122i & 0.0000+0.0000i \\ 0.0000+0.0000i & 0.0848-0.0492i & -0.2939+0.1703i & 0.0000+0.0000i \\ 0.0000+0.0000i & 0.1813+0.0748i & 0.0973-0.3103i & 0.0000+0.0000i \\ 0.0000+0.0000i & -0.0720-0.1538i & -0.1314-0.2809i & 0.0000+0.0000i \\ 0.0000+0.0000i & -0.0848+0.0492i & 0.2939-0.1703i & 0.0000+0.0000i \\ 0.0000+0.0000i & -0.0415+0.1323i & -0.2719-0.1122i & 0.0000+0.0000i \end{bmatrix}^H$$

transmission power or bandwidth. This is an encouraging discovery.

Indeed, in order to achieve VBR codebooks, we need to pay a certain price. First, there will be several reserve

$$\mathcal{X}_1: \begin{bmatrix} 0.0121+0.1381i & 0.0284+0.3240i & 0.0000+0.0000i & 0.0000+0.0000i \\ 0.0723+0.0662i & -0.2505-0.2295i & 0.0000+0.0000i & 0.0000+0.0000i \\ -0.0723-0.0662i & 0.2505+0.2295i & 0.0000+0.0000i & 0.0000+0.0000i \\ -0.0121-0.1381i & -0.0284-0.3240i & 0.0000+0.0000i & 0.0000+0.0000i \\ 0.1033-0.1348i & -0.1887+0.2461i & 0.0000+0.0000i & 0.0000+0.0000i \\ -0.1931+0.0342i & -0.2897+0.0512i & 0.0000+0.0000i & 0.0000+0.0000i \\ 0.1931-0.0342i & 0.2897-0.0512i & 0.0000+0.0000i & 0.0000+0.0000i \\ -0.1033+0.1348i & 0.1887-0.2461i & 0.0000+0.0000i & 0.0000+0.0000i \end{bmatrix}^H$$

$$\mathcal{X}_2: \begin{bmatrix} 0.0000+0.0000i & 0.0000+0.0000i & 0.0121+0.1381i & 0.0284+0.3240i \\ 0.0000+0.0000i & 0.0000+0.0000i & 0.0723+0.0662i & -0.2505-0.2295i \\ 0.0000+0.0000i & 0.0000+0.0000i & -0.0723-0.0662i & 0.2505+0.2295i \\ 0.0000+0.0000i & 0.0000+0.0000i & -0.0121-0.1381i & -0.0284-0.3240i \\ 0.0000+0.0000i & 0.0000+0.0000i & 0.1033-0.1348i & -0.1887+0.2461i \\ 0.0000+0.0000i & 0.0000+0.0000i & -0.1931+0.0342i & -0.2897+0.0512i \\ 0.0000+0.0000i & 0.0000+0.0000i & 0.1931-0.0342i & 0.2897-0.0512i \\ 0.0000+0.0000i & 0.0000+0.0000i & -0.1033+0.1348i & 0.1887-0.2461i \end{bmatrix}^H$$

$$\mathcal{X}_3: \begin{bmatrix} -0.0624-0.2320i & 0.0000+0.0000i & -0.0674-0.2505i & 0.0000+0.0000i \\ 0.1850+0.1177i & 0.0000+0.0000i & -0.2340-0.1489i & 0.0000+0.0000i \\ -0.1850-0.1177i & 0.0000+0.0000i & 0.2340+0.1489i & 0.0000+0.0000i \\ 0.0624+0.2320i & 0.0000+0.0000i & 0.0674+0.2505i & 0.0000+0.0000i \\ 0.1196-0.2302i & 0.0000+0.0000i & -0.1107+0.2132i & 0.0000+0.0000i \\ 0.2605-0.0951i & 0.0000+0.0000i & 0.2060-0.0752i & 0.0000+0.0000i \\ -0.2605+0.0951i & 0.0000+0.0000i & -0.2060+0.0752i & 0.0000+0.0000i \\ -0.1196+0.2302i & 0.0000+0.0000i & 0.1107-0.2132i & 0.0000+0.0000i \end{bmatrix}^H$$

$$\mathcal{X}_4: \begin{bmatrix} 0.0000+0.0000i & -0.0624-0.2320i & 0.0000+0.0000i & -0.0674-0.2505i \\ 0.0000+0.0000i & 0.1850+0.1177i & 0.0000+0.0000i & -0.2340-0.1489i \\ 0.0000+0.0000i & -0.1850-0.1177i & 0.0000+0.0000i & 0.2340+0.1489i \\ 0.0000+0.0000i & 0.0624+0.2320i & 0.0000+0.0000i & 0.0674+0.2505i \\ 0.0000+0.0000i & 0.1196-0.2302i & 0.0000+0.0000i & -0.1107+0.2132i \\ 0.0000+0.0000i & 0.2605-0.0951i & 0.0000+0.0000i & 0.2060-0.0752i \\ 0.0000+0.0000i & -0.2605+0.0951i & 0.0000+0.0000i & -0.2060+0.0752i \\ 0.0000+0.0000i & -0.1196+0.2302i & 0.0000+0.0000i & 0.1107-0.2132i \end{bmatrix}^H$$

$$\mathcal{X}_5: \begin{bmatrix} 0.2939-0.1703i & 0.0000+0.0000i & 0.0000+0.0000i & 0.0848-0.0492i \\ -0.0973+0.3103i & 0.0000+0.0000i & 0.0000+0.0000i & 0.0415-0.1323i \\ 0.0973-0.3103i & 0.0000+0.0000i & 0.0000+0.0000i & -0.0415+0.1323i \\ -0.2939+0.1703i & 0.0000+0.0000i & 0.0000+0.0000i & -0.0848+0.0492i \\ 0.2719+0.1122i & 0.0000+0.0000i & 0.0000+0.0000i & -0.1813-0.0748i \\ 0.1314+0.2809i & 0.0000+0.0000i & 0.0000+0.0000i & 0.0720+0.1538i \\ -0.1314-0.2809i & 0.0000+0.0000i & 0.0000+0.0000i & -0.0720-0.1538i \\ -0.2719-0.1122i & 0.0000+0.0000i & 0.0000+0.0000i & 0.1813+0.0748i \end{bmatrix}^H$$

$$\mathcal{X}_6: \begin{bmatrix} 0.0000+0.0000i & 0.0848-0.0492i & 0.2939-0.1703i & 0.0000+0.0000i \\ 0.0000+0.0000i & 0.0415-0.1323i & -0.0973+0.3103i & 0.0000+0.0000i \\ 0.0000+0.0000i & -0.0415+0.1323i & 0.0973-0.3103i & 0.0000+0.0000i \\ 0.0000+0.0000i & -0.0848+0.0492i & -0.2939+0.1703i & 0.0000+0.0000i \\ 0.0000+0.0000i & -0.1813-0.0748i & 0.2719+0.1122i & 0.0000+0.0000i \\ 0.0000+0.0000i & 0.0720+0.1538i & 0.1314+0.2809i & 0.0000+0.0000i \\ 0.0000+0.0000i & -0.0720-0.1538i & -0.1314-0.2809i & 0.0000+0.0000i \\ 0.0000+0.0000i & 0.1813+0.0748i & -0.2719-0.1122i & 0.0000+0.0000i \end{bmatrix}^H$$

$$\mathcal{X}_1: \begin{bmatrix} 0.0623+0.0571i & 0.2332+0.2136i & 0.0000+0.0000i & 0.0000+0.0000i \\ -0.0623-0.0571i & -0.2332-0.2136i & 0.0000+0.0000i & 0.0000+0.0000i \\ 0.0104+0.1191i & 0.0266+0.3036i & 0.0000+0.0000i & 0.0000+0.0000i \\ -0.0104-0.1191i & -0.0266-0.3036i & 0.0000+0.0000i & 0.0000+0.0000i \end{bmatrix}^H$$

$$\mathcal{X}_2: \begin{bmatrix} 0.0000+0.0000i & 0.0000+0.0000i & 0.0623+0.0571i & 0.2332+0.2136i \\ 0.0000+0.0000i & 0.0000+0.0000i & -0.0623-0.0571i & -0.2332-0.2136i \\ 0.0000+0.0000i & 0.0000+0.0000i & 0.0104+0.1191i & 0.0266+0.3036i \\ 0.0000+0.0000i & 0.0000+0.0000i & -0.0104-0.1191i & -0.0266-0.3036i \end{bmatrix}^H$$

$$\mathcal{X}_3: \begin{bmatrix} -0.1595-0.1014i & 0.0000+0.0000i & -0.2255-0.1434i & 0.0000+0.0000i \\ -0.1664+0.0294i & 0.0000+0.0000i & -0.2760+0.0488i & 0.0000+0.0000i \\ 0.1664-0.0294i & 0.0000+0.0000i & 0.2760-0.0488i & 0.0000+0.0000i \\ 0.1595+0.1014i & 0.0000+0.0000i & 0.2255+0.1434i & 0.0000+0.0000i \\ -0.0537-0.1999i & 0.0000+0.0000i & -0.0658-0.2449i & 0.0000+0.0000i \\ -0.0891+0.1162i & 0.0000+0.0000i & -0.1781+0.2323i & 0.0000+0.0000i \\ 0.0891-0.1162i & 0.0000+0.0000i & 0.1781-0.2323i & 0.0000+0.0000i \\ 0.0537+0.1999i & 0.0000+0.0000i & 0.0658+0.2449i & 0.0000+0.0000i \end{bmatrix}^H$$

$$\mathcal{X}_4: \begin{bmatrix} 0.0000+0.0000i & -0.1595-0.1014i & 0.0000+0.0000i & -0.2255-0.1434i \\ 0.0000+0.0000i & -0.1664+0.0294i & 0.0000+0.0000i & -0.2760+0.0488i \\ 0.0000+0.0000i & 0.1664-0.0294i & 0.0000+0.0000i & 0.2760-0.0488i \\ 0.0000+0.0000i & 0.1595+0.1014i & 0.0000+0.0000i & 0.2255+0.1434i \\ 0.0000+0.0000i & -0.0537-0.1999i & 0.0000+0.0000i & -0.0658-0.2449i \\ 0.0000+0.0000i & -0.0891+0.1162i & 0.0000+0.0000i & -0.1781+0.2323i \\ 0.0000+0.0000i & 0.0891-0.1162i & 0.0000+0.0000i & 0.1781-0.2323i \\ 0.0000+0.0000i & 0.0537+0.1999i & 0.0000+0.0000i & 0.0658+0.2449i \end{bmatrix}^H$$

$$\mathcal{X}_5: \begin{bmatrix} 0.0839-0.2675i & 0.0000+0.0000i & 0.0000+0.0000i & 0.0506-0.1613i \\ -0.2245+0.0820i & 0.0000+0.0000i & 0.0000+0.0000i & -0.2100+0.0767i \\ 0.1031-0.1984i & 0.0000+0.0000i & 0.0000+0.0000i & 0.1102-0.2121i \\ -0.0839+0.2675i & 0.0000+0.0000i & 0.0000+0.0000i & -0.0506+0.1613i \\ -0.1819-0.2587i & 0.0000+0.0000i & 0.0000+0.0000i & -0.0486-0.0691i \\ -0.2344-0.0967i & 0.0000+0.0000i & 0.0000+0.0000i & -0.1914-0.0790i \\ -0.1133-0.2421i & 0.0000+0.0000i & 0.0000+0.0000i & -0.0801-0.1712i \\ 0.1133+0.2421i & 0.0000+0.0000i & 0.0000+0.0000i & 0.0801+0.1712i \\ 0.2245-0.0820i & 0.0000+0.0000i & 0.0000+0.0000i & 0.2100-0.0767i \\ -0.2533+0.1468i & 0.0000+0.0000i & 0.0000+0.0000i & -0.1267+0.0734i \\ 0.2533-0.1468i & 0.0000+0.0000i & 0.0000+0.0000i & 0.1267-0.0734i \\ -0.1031+0.1984i & 0.0000+0.0000i & 0.0000+0.0000i & -0.1102+0.2121i \\ 0.2976+0.0654i & 0.0000+0.0000i & 0.0000+0.0000i & 0.1167+0.0257i \\ -0.2976-0.0654i & 0.0000+0.0000i & 0.0000+0.0000i & -0.1167-0.0257i \\ 0.2344+0.0967i & 0.0000+0.0000i & 0.0000+0.0000i & 0.1914+0.0790i \\ 0.1819+0.2587i & 0.0000+0.0000i & 0.0000+0.0000i & 0.0486+0.0691i \end{bmatrix}^H$$

$$\mathcal{X}_6: \begin{bmatrix} 0.0000+0.0000i & 0.0839-0.2675i & 0.0506-0.1613i & 0.0000+0.0000i \\ 0.0000+0.0000i & -0.2245+0.0820i & -0.2100+0.0767i & 0.0000+0.0000i \\ 0.0000+0.0000i & 0.1031-0.1984i & 0.1102-0.2121i & 0.0000+0.0000i \\ 0.0000+0.0000i & -0.0839+0.2675i & -0.0506+0.1613i & 0.0000+0.0000i \\ 0.0000+0.0000i & -0.1819-0.2587i & -0.0486-0.0691i & 0.0000+0.0000i \\ 0.0000+0.0000i & -0.2344-0.0967i & -0.1914-0.0790i & 0.0000+0.0000i \\ 0.0000+0.0000i & -0.1133-0.2421i & -0.0801-0.1712i & 0.0000+0.0000i \\ 0.0000+0.0000i & 0.1133+0.2421i & 0.0801+0.1712i & 0.0000+0.0000i \\ 0.0000+0.0000i & 0.2245-0.0820i & 0.2100-0.0767i & 0.0000+0.0000i \\ 0.0000+0.0000i & -0.2533+0.1468i & -0.1267+0.0734i & 0.0000+0.0000i \\ 0.0000+0.0000i & 0.2533-0.1468i & 0.1267-0.0734i & 0.0000+0.0000i \\ 0.0000+0.0000i & -0.1031+0.1984i & -0.1102+0.2121i & 0.0000+0.0000i \\ 0.0000+0.0000i & 0.2976+0.0654i & 0.1167+0.0257i & 0.0000+0.0000i \\ 0.0000+0.0000i & -0.2976-0.0654i & -0.1167-0.0257i & 0.0000+0.0000i \\ 0.0000+0.0000i & 0.2344+0.0967i & 0.1914+0.0790i & 0.0000+0.0000i \\ 0.0000+0.0000i & 0.1819+0.2587i & 0.0486+0.0691i & 0.0000+0.0000i \end{bmatrix}^H$$

$$\mathcal{X}_1: \begin{bmatrix} 0.0623+0.0571i & 0.2332+0.2136i & 0.0000+0.0000i & 0.0000+0.0000i \\ -0.0623-0.0571i & -0.2332-0.2136i & 0.0000+0.0000i & 0.0000+0.0000i \\ 0.0104+0.1191i & 0.0266+0.3036i & 0.0000+0.0000i & 0.0000+0.0000i \\ -0.0104-0.1191i & -0.0266-0.3036i & 0.0000+0.0000i & 0.0000+0.0000i \end{bmatrix}^H$$

$$\mathcal{X}_2: \begin{bmatrix} 0.0000+0.0000i & 0.0000+0.0000i & 0.0623+0.0571i & 0.2332+0.2136i \\ 0.0000+0.0000i & 0.0000+0.0000i & -0.0623-0.0571i & -0.2332-0.2136i \\ 0.0000+0.0000i & 0.0000+0.0000i & 0.0104+0.1191i & 0.0266+0.3036i \\ 0.0000+0.0000i & 0.0000+0.0000i & -0.0104-0.1191i & -0.0266-0.3036i \end{bmatrix}^H$$

$$\mathcal{X}_3: \begin{bmatrix} -0.1595-0.1014i & 0.0000+0.0000i & -0.2255-0.1434i & 0.0000+0.0000i \\ -0.1664+0.0294i & 0.0000+0.0000i & -0.2760+0.0488i & 0.0000+0.0000i \\ -0.0537-0.1999i & 0.0000+0.0000i & -0.0658-0.2449i & 0.0000+0.0000i \\ -0.0891+0.1162i & 0.0000+0.0000i & -0.1781+0.2323i & 0.0000+0.0000i \\ 0.1664-0.0294i & 0.0000+0.0000i & 0.2760-0.0488i & 0.0000+0.0000i \\ 0.1595+0.1014i & 0.0000+0.0000i & 0.2255+0.1434i & 0.0000+0.0000i \\ 0.0891-0.1162i & 0.0000+0.0000i & 0.1781-0.2323i & 0.0000+0.0000i \\ 0.0537+0.1999i & 0.0000+0.0000i & 0.0658+0.2449i & 0.0000+0.0000i \end{bmatrix}^H$$

$$\mathcal{X}_4: \begin{bmatrix} 0.0000+0.0000i & -0.1595-0.1014i & 0.0000+0.0000i & -0.2255-0.1434i \\ 0.0000+0.0000i & -0.1664+0.0294i & 0.0000+0.0000i & -0.2760+0.0488i \\ 0.0000+0.0000i & -0.0537-0.1999i & 0.0000+0.0000i & -0.0658-0.2449i \\ 0.0000+0.0000i & -0.0891+0.1162i & 0.0000+0.0000i & -0.1781+0.2323i \\ 0.0000+0.0000i & 0.1664-0.0294i & 0.0000+0.0000i & 0.2760-0.0488i \\ 0.0000+0.0000i & 0.1595+0.1014i & 0.0000+0.0000i & 0.2255+0.1434i \\ 0.0000+0.0000i & 0.0891-0.1162i & 0.0000+0.0000i & 0.1781-0.2323i \\ 0.0000+0.0000i & 0.0537+0.1999i & 0.0000+0.0000i & 0.0658+0.2449i \end{bmatrix}^H$$

$$\mathcal{X}_5: \begin{bmatrix} 0.2533-0.1468i & 0.0000+0.0000i & 0.0000+0.0000i & 0.1267-0.0734i \\ -0.0839+0.2675i & 0.0000+0.0000i & 0.0000+0.0000i & -0.0506+0.1613i \\ 0.2245-0.0820i & 0.0000+0.0000i & 0.0000+0.0000i & 0.2100-0.0767i \\ -0.1031+0.1984i & 0.0000+0.0000i & 0.0000+0.0000i & -0.1102+0.2121i \\ 0.2976+0.0654i & 0.0000+0.0000i & 0.0000+0.0000i & 0.1167+0.0257i \\ 0.1819+0.2587i & 0.0000+0.0000i & 0.0000+0.0000i & 0.0486+0.0691i \\ 0.2344+0.0967i & 0.0000+0.0000i & 0.0000+0.0000i & 0.1914+0.0790i \\ 0.1133+0.2421i & 0.0000+0.0000i & 0.0000+0.0000i & 0.0801+0.1712i \\ 0.1031-0.1984i & 0.0000+0.0000i & 0.0000+0.0000i & 0.1102-0.2121i \\ -0.2245+0.0820i & 0.0000+0.0000i & 0.0000+0.0000i & -0.2100+0.0767i \\ 0.0839-0.2675i & 0.0000+0.0000i & 0.0000+0.0000i & 0.0506-0.1613i \\ -0.2533+0.1468i & 0.0000+0.0000i & 0.0000+0.0000i & -0.1267+0.0734i \\ -0.1133-0.2421i & 0.0000+0.0000i & 0.0000+0.0000i & -0.0801-0.1712i \\ -0.2344-0.0967i & 0.0000+0.0000i & 0.0000+0.0000i & -0.1914-0.0790i \\ -0.1819-0.2587i & 0.0000+0.0000i & 0.0000+0.0000i & -0.0486-0.0691i \\ -0.2976-0.0654i & 0.0000+0.0000i & 0.0000+0.0000i & -0.1167-0.0257i \end{bmatrix}^H$$

$$\mathcal{X}_6: \begin{bmatrix} 0.0000+0.0000i & 0.2533-0.1468i & 0.1267-0.0734i & 0.0000+0.0000i \\ 0.0000+0.0000i & -0.0839+0.2675i & -0.0506+0.1613i & 0.0000+0.0000i \\ 0.0000+0.0000i & 0.2245-0.0820i & 0.2100-0.0767i & 0.0000+0.0000i \\ 0.0000+0.0000i & -0.1031+0.1984i & -0.1102+0.2121i & 0.0000+0.0000i \\ 0.0000+0.0000i & 0.2976+0.0654i & 0.1167+0.0257i & 0.0000+0.0000i \\ 0.0000+0.0000i & 0.1819+0.2587i & 0.0486+0.0691i & 0.0000+0.0000i \\ 0.0000+0.0000i & 0.2344+0.0967i & 0.1914+0.0790i & 0.0000+0.0000i \\ 0.0000+0.0000i & 0.1133+0.2421i & 0.0801+0.1712i & 0.0000+0.0000i \\ 0.0000+0.0000i & 0.1031-0.1984i & 0.1102-0.2121i & 0.0000+0.0000i \\ 0.0000+0.0000i & -0.2245+0.0820i & -0.2100+0.0767i & 0.0000+0.0000i \\ 0.0000+0.0000i & 0.0839-0.2675i & 0.0506-0.1613i & 0.0000+0.0000i \\ 0.0000+0.0000i & -0.2533+0.1468i & -0.1267+0.0734i & 0.0000+0.0000i \\ 0.0000+0.0000i & -0.1133-0.2421i & -0.0801-0.1712i & 0.0000+0.0000i \\ 0.0000+0.0000i & -0.2344-0.0967i & -0.1914-0.0790i & 0.0000+0.0000i \\ 0.0000+0.0000i & -0.1819-0.2587i & -0.0486-0.0691i & 0.0000+0.0000i \\ 0.0000+0.0000i & -0.2976-0.0654i & -0.1167-0.0257i & 0.0000+0.0000i \end{bmatrix}^H$$

codebooks with different modulation order in the system. The reserve codebooks also need to be considered at the beginning of the design. According to the design produce, this will increase the scale of the GAM constellation with higher power. And then, the power of each codeword in each codebook will increase correspondingly. Second, the users employing VBR codebooks with small modulation order has a lower power efficiency compared with the users employing CBR codebooks. On the contrary, the users employing VBR codebooks with large modulation order has a higher power efficiency compared with the users employing CBR codebooks. That is to say, we sacrifice power efficiency to realize variable rate codebook. Furthermore, any user can't change the power of the transmitted symbol at will, because this operation will affect the MPD and MED of the superposition symbols making them more difficult to distinguish. All these interfering users should control the transmission power in coordination to increase the MED and MPD of superposition symbols/codewords, so as to improve the system performance. This feature shows that the SCMA is a cooperative communication system.

VI. CONCLUSION

In this study, we propose a DEMC method to construct the SCMA codebooks simply and efficiently. Compared with the previous work, we abandon those optimization steps, such as optimizing rotation angle, MED, and MPD which result in an unreachable computational complexity with the increase of codebook scale. On the contrary, we introduce the power and phase dependence constraints between different dimensions in codewords. Based on the DEMC method, we construct CBR and VBR SCMA codebooks that can flexibly satisfy the application requirements. Simulations show that the BER performance of the proposed SCMA codebooks is outstanding with low complexity. The BER performance of the VBR codebooks is close to each other though their modulation orders are various. Given the outstanding performance and low complexity of DEMC-SCMA codebooks, it is reasonable to be developed for the large scale codebooks design. Next, we will study the spreading gain (SG) of the codebook based on the power and phase dependence. After all, the SCMA is a sparse spread spectrum communication system like the CDMA.

.

APPENDIX A CODEBOOKS USED IN THIS STUDY

A. Codebooks used in Fig.4. $\mathcal{X}_1$–$\mathcal{X}_6$, as shown at the bottom of the 9th page.

B. Codebooks used in Fig.5. $\mathcal{X}_1$–$\mathcal{X}_6$, as shown at the bottom of the 10th page.

C. Codebooks used in Fig.6 and Fig.7 for AWGN channel. $\mathcal{X}_1$–$\mathcal{X}_6$, as shown at the bottom of the 11th page.

D. Codebooks used in Fig.6 and Fig.8 for Rayleigh channel. $\mathcal{X}_1$–$\mathcal{X}_6$, as shown at the bottom of the 12th page.

REFERENCES

[1] H. Nikopour and H. Baligh, "Sparse code multiple access," in *Proc. IEEE 24th Annu. Int. Symp. Pers., Indoor, Mobile Radio Commun. (PIMRC)*, Sep. 2013, pp. 332–336.

[2] L. Wang, X. Xu, Y. Wu, S. Xing, and Y. Chen, "Sparse code multiple access-towards massive connectivity and low latency 5G communications," *Telecommun. Netw. Technol.*, vol. 4, no. 5, pp. 6–15, 2015.

[3] J. van de Beek and B. M. Popovic, "Multiple access with low-density signatures," in *Proc. IEEE Global Telecommun. Conf.*, Oct. 2009, pp. 1–6.

[4] H. Nikopour and M. Baligh, "Systems and methods for sparse code multiple access," Tech. Rep., 2016.

[5] S. Zhang, X. Xu, L. Lu, Y. Wu, G. He, and Y. Chen, "Sparse code multiple access: An energy efficient uplink approach for 5G wireless systems," in *Proc. IEEE Global Commun. Conf.*, Dec. 2014, pp. 4782–4787.

[6] H. Nikopour, E. Yi, A. Bayesteh, K. Au, M. Hawryluck, H. Baligh, and J. Ma, "SCMA for downlink multiple access of 5G wireless networks," in *Proc. IEEE Global Commun. Conf.*, Dec. 2014, pp. 3940–3945.

[7] Y. Tao, L. Liu, S. Liu, and Z. Zhang, "A survey: Several technologies of non-orthogonal transmission for 5G," *China Commun.*, vol. 12, no. 10, pp. 1–15, Oct. 2015.

[8] G. D. Forney and L. F. Wei, "Multidimensional constellations—Part I: Introduction. figures of merit, and generalized cross constellations," *IEEE J. Sel. Areas Commun.*, vol. 7, no. 6, pp. 877–892, Oct. 1989.

[9] M. Beko and R. Dinis, "Designing good multi-dimensional constellations," *IEEE Wireless Commun. Lett.*, vol. 1, no. 3, pp. 221–224, Jun. 2012.

[10] H. Wu, J. Zhang, and H. Song, "A lattice based approach to the construction of multi-dimensional signal constellations," *ACTC Electronica Sinica.*, vol. 42, no. 9, pp. 1672–1679, 2014.

[11] M. Taherzadeh, H. Nikopour, A. Bayesteh, and H. Baligh, "SCMA codebook design," in *Proc. IEEE 80th Veh. Technol. Conf. (VTC-Fall)*, Sep. 2014, pp. 1–5.

[12] C. Yan, G. Kang, and N. Zhang, "A dimension distance-based SCMA codebook design," *IEEE Access*, vol. 5, pp. 5471–5479, 2017.

[13] S. Zhang, K. Xiao, B. Xiao, Z. Chen, B. Xia, D. Chen, and S. Ma, "A capacity-based codebook design method for sparse code multiple access systems," in *Proc. 8th Int. Conf. Wireless Commun. Signal Process. (WCSP)*, Oct. 2016, pp. 1–5.

[14] L. Yu, X. Lei, P. Fan, and D. Chen, "An optimized design of SCMA codebook based on star-QAM signaling constellations," in *Proc. Int. Conf. Wireless Commun. Signal Process. (WCSP)*, Oct. 2015, pp. 1–5.

[15] D. Cai, P. Fan, X. Lei, Y. Liu, and D. Chen, "Multi-dimensional SCMA codebook design based on constellation rotation and interleaving," in *Proc. IEEE 83rd Veh. Technol. Conf. (VTC Spring)*, May 2016, pp. 1–5.

[16] S. Liu, J. Wang, J. Bao, and C. Liu, "Optimized scma codebook design by qam constellation segmentation with maximized med," *IEEE Access*, vol. 6, pp. 63232–63242, 2018.

[17] Z. Mheich, L. Wen, P. Xiao, and A. Maaref, "Design of SCMA codebooks based on golden angle modulation," *IEEE Trans. Veh. Technol.*, vol. 68, no. 2, pp. 1501–1509, Feb. 2019.

[18] Y.-M. Chen and J.-W. Chen, "On the design of near-optimal sparse code multiple access codebooks," *IEEE Trans. Commun.*, vol. 68, no. 5, pp. 2950–2962, May 2020.

[19] X. Zhang, G. Han, D. Zhang, D. Zhang, and L. Yang, "An efficient scma codebook design based on lattice theory for information-centric iot," *IEEE Access*, vol. 7, pp. 133865–133875, 2019.

[20] J. Zou, H. Zhao, and W. Zhao, "Low-complexity interference cancellation receiver for sparse code multiple access," in *2015 IEEE 6th Int. Symp. Microw., Antenna, Propag., EMC Technol. (MAPE)*, 2015, pp. 277–282.

[21] A. Ghaffari, M. Leonardon, Y. Savaria, C. Jego, and C. Leroux, "Improving performance of SCMA MPA decoders using estimation of conditional probabilities," in *Proc. 15th IEEE Int. New Circuits Syst. Conf. (NEWCAS)*, Jun. 2017, pp. 21–24.

[22] K. Xiao, B. Xiao, S. Zhang, Z. Chen, and B. Xia, "Simplified multiuser detection for SCMA with sum-product algorithm," in *Proc. Int. Conf. Wireless Commun. Signal Process. (WCSP)*, Oct. 2015, pp. 1–5.

[23] Z. Liu and L.-L. Yang, "Sparse or dense: A comparative study of code-domain NOMA systems," *IEEE Trans. Wireless Commun.*, early access, Mar. 4, 2021, doi: 10.1109/TWC.2021.3062235.

[24] Z. Mheich, Z. Liu, P. Xiao, and A. Maaref, "Delayed bit interleaved coded sparse code multiple access," *IEEE Trans. Veh. Technol.*, vol. 69, no. 7, pp. 8018–8022, Jul. 2020.

[25] Z. Liu, P. Xiao, and Z. Mheich, "Power-imbalanced low-density signatures (LDS) from eisenstein numbers," in *Proc. IEEE VTS Asia Pacific Wireless Commun. Symp. (APWCS)*, Aug. 2019, pp. 1–5.

[26] P. Larsson, "Golden angle modulation," *IEEE Wireless Commun. Lett.*, vol. 7, no. 1, pp. 98–101, Feb. 2018.
[27] P. Larsson, L. K. Rasmussen, and M. Skoglund, "Golden angle modulation: Approaching the AWGN capacity," 2018, *arXiv:1802.10022*. [Online]. Available: http://arxiv.org/abs/1802.10022
[28] P. Larsson, "Golden angle modulation: Geometric- and probabilistic-shaping," 2017, *arXiv:1708.07321*. [Online]. Available: http://arxiv.org/abs/1708.07321
[29] Y. Zhi-Hua, H. Li-Mei, and T. Xiao-Bao, "Performance study for golden angle modulation in SM-MIMO system," *Modern Comput.*, no. 13, pp. 9–12, 2019.
[30] I. Yildirim, E. Basar, and I. Altunbas, "Fractional media-based modulation with golden angle modulation," in *Proc. IEEE Wireless Commun. Netw. Conf. Workshop (WCNCW)*, Apr. 2019, pp. 1–5.
[31] F. R. Kschischang, B. J. Frey, and H.-A. Loeliger, "Factor graphs and the sum-product algorithm," *IEEE Trans. Inf. Theory*, vol. 47, no. 2, pp. 498–519, Mar. 2001.
[32] L. Wang, D. Xu, and X. Zhang, "Recursive bit metric generation for PSK signals with gray labeling," *IEEE Commun. Lett.*, vol. 16, no. 2, pp. 180–182, Feb. 2012.
[33] F. Schreckenbach, N. Gortz, J. Hagenauer, and G. Bauch, "Optimization of symbol mappings for bit-interleaved coded modulation with iterative decoding," *IEEE Commun. Lett.*, vol. 7, no. 12, pp. 593–595, Dec. 2003.

ZHAOYANG HOU received the B.S. degree from the School of Information Engineering, Tianjin University of Commerce, Tianjin, China, in 2013, and the M.S. degree from the School of Information Engineering, Zhengzhou University, Zhengzhou, China, in 2016. He is currently pursuing the Ph.D. degree in science of military command with Xidian University, Xi'an, China. His research interests include signal processing and wireless communication systems.

ZHENG XIANG received the B.S. and M.S. degrees from Air Force Engineering University, Xi'an, China, in 1990 and 1993, respectively, and the Ph.D. degree from Xi'an Jiaotong University, Xi'an, in 2006. Since 2001, he has been a Faculty Member with the School of Telecommunications Engineering, Xidian University, where he is currently a Full Professor with the State Key Laboratory of Integrated Services Networks. His current research interests include signal processing technologies, self-organizing networks, and wireless sensor networks.

PENG REN received the B.S., M.S., and Ph.D. degrees in telecommunications engineering from Xidian University, Xi'an, China, in 2006, 2010, and 2014, respectively. He is currently working as an Associate Professor with the School of Telecommunications Engineering, Xidian University. His current research interests include wireless communication theory, signal processing technologies, and the Internet of Things.

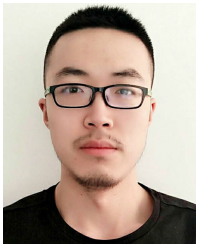

BOHAO CAO received the B.S. degree in telecommunication engineering from Xidian University, Xi'an, China, in 2018, where he is currently pursuing the Ph.D. degree in science of military command with the School of Telecommunications Engineering. His research interests include OTFS, array signal processing, and broadband data communication.